

# Flourescent Probe and ESEM Morphologies of a Acrylamide-Based Terpolymer in Aqueous Solution

Chuanrong Zhong,<sup>1-3</sup> Lin Ye,<sup>2</sup> Hua Dai,<sup>2</sup> Ronghua Huang<sup>2</sup>

<sup>1</sup>Materials and Chemistry Chemical Engineering College, Chengdu University of Technology, Chengdu 610059, Sichuan Province, China

<sup>2</sup>The State Key Laboratory of Polymer Materials Engineering, Polymer Research Institute, Sichuan University, Chengdu 610065, Sichuan Province, China

<sup>3</sup>The State Key Laboratory of Oil and Gas Reservoir Geology and Exploitation, Southwest Petroleum Institute, Chengdu 610500, Sichuan Province, China

Received 14 November 2005; accepted 17 August 2006

DOI 10.1002/app.25275

Published online in Wiley InterScience (www.interscience.wiley.com).

**ABSTRACT:** The terpolymer (PASA) of acrylamide with butyl styrene and sodium 2-acrylamido-2-methylpropane sulfonate was synthesized. The composition and molecular structure were characterized by elemental analysis, UV, FTIR, and <sup>1</sup>H NMR. The aggregation behaviors of PASA were studied by means of the flourescent probe analysis and environmental scanning electron microscope (ESEM). The flourescent probe analysis indicates that the PASA molecules form excellent hydrophobically associating structures in pure water and with the increase in PASA concentration at low concentrations, the nonpolarity of hydrophobic microdomains and the degree of intermolecular hydrophobic association increase in aqueous and brine solution. ESEM measurements show that gigantic aggregates have been formed in the PASA aqueous solution at the polymer concentration of 0.05 g dL<sup>-1</sup>, which is the critical associa-

tion concentration of the polymer, and excellent solution properties of PASA are attributed to integrated network-structures formed by PASA in aqueous solution, which are collapsed by the addition of salt, resulting in the decrease in apparent viscosity of PASA in brine solution. However, with the increase in the NaCl concentration or the PASA concentration, the number and size of aggregates increase, leading to the remarkable increase in the apparent viscosity of PASA in brine solution. These results are consistent with the AFM and viscosity study results. © 2006 Wiley Periodicals, Inc. *J Appl Polym Sci* 103: 277–286, 2007

**Key words:** hydrophobically associating water-soluble polymer; aggregation morphology; environmental scanning electron microscope; fluorescent probe

## INTRODUCTION

Hydrophobically associating water-soluble polymers are water-soluble polymers containing a small amount of hydrophobic groups. When dissolved in water, above the critical concentration ( $C^*$ ), the hydrophobic groups can associate together via intra- and intermolecular interaction to form physical network structures, which are reversible and different from cross-linked structures formed by covalent bonds, resulting in substantial viscosity increase. Upon application of shear, the network structures are disrupted, showing typical pseudoplastic behavior. However, upon the removal of shear, the associations and network struc-

tures can reform and the viscosities of polymer solutions completely recover their original values. Because of these unique solution properties, the hydrophobically associating polymers have been widely applied in enhanced oil recovery (EOR), drag reduction, flocculation, cosmetics, and so on.<sup>1-4</sup>

Presently, numerous studies on hydrophobically modified polymers have been concentrated on the copolymers containing acrylamide (AM) and a hydrophobic monomer, which are commonly the derivatives of AM, acrylic esters, and its derivatives,<sup>5-9</sup> and are easy to hydrolyze under acidic or basic conditions at high temperature, resulting in the abrupt decrease in the viscosities of the polymer solution. These kinds of copolymers are difficult to dissolve in water, and the viscosities at low polymer concentration are not high enough to be applied in some areas, especially in EOR with high temperature and nonneutral underground oil layer environment.<sup>10,11</sup> To obtain the polymeric thickener used as the oil-displacement agent with good solution properties such as high viscosity, salt-thickening, antishearing, and antiageing, the AFM

Correspondence to: C. Zhong (zhchrong2006@yahoo.com.cn).

Contract grant sponsor: Research Fund of Chengdu University of Technology; contract grant number: 2004YG01.

Contract grant sponsor: National 973 Project; contract grant number: G1999022502.

measurements and viscosity study were reported for the novel terpolymer (PASA) containing AM, butyl styrene (BST) as the hydrophobic monomer, and sodium 2-acrylamido-2-methylpropane sulfonate (NaAMPS).<sup>12</sup> The phenyl group from BST is well-known to induce van der Waals interaction due to its plane and polarizable structure, and improve the rigidity of hydrophobic unit. Thus, the incorporation of such group into the copolymer leads to the enhancement of the intermolecular hydrophobic interaction and high viscosity values of the polymer solution at a low polymer concentration, and the phenyl groups linked directly with main chains can also stabilize the hydrophobic units.<sup>13</sup> The water-solubility of the polymer has been improved by incorporating the anionic groups of NaAMPS monomer into the molecules of PASA. This study aims to characterize PASA by elemental analysis, UV, FTIR, and <sup>1</sup>H NMR, and study the polarity of hydrophobic microdomains in the aqueous and brine solution of PASA by the measurements of fluorescent probe. In addition, the natural associating morphologies of the polymer were directly observed by environmental scanning electron microscope (ESAM) to reveal the relationship between viscosification properties and microstructures of the hydrophobically associating water-soluble polymers in aqueous and brine solution.

## EXPERIMENTAL

### Reagents

AM was recrystallized twice from CHCl<sub>3</sub>, and 2-acrylamido-2-methylpropane sulfonate (AMPS) was purchased from Lubrizol, and used directly. Butyl styrene (BST) was prepared in the laboratory.<sup>14</sup> Other reagents were analytically pure and used without further purification.

### Synthesis of copolymers

The PASA terpolymers were prepared by the free radical micellar copolymerization<sup>15,16</sup> using sodium dodecyl sulfate (SDS) as the surfactant and potassium persulphate as the initiator. The typical micellar copolymerization process is as follows. A 100-mL, three-necked, round flask was equipped with a mechanical stirrer, nitrogen inlet, and outlet. Four grams (0.0563 mol) AM, 1.31 g ( $6.326 \times 10^{-3}$  mol) AMPS, 2.88 g SDS, and 47.79 g distilled water were added, respectively, into the reaction flask and NaOH was used to control the pH value of the reaction solution within 6–7. The mixture was stirred for 15 min, and then 0.25 g ( $1.566 \times 10^{-3}$  mol) BST was added into the reaction flask. The flask was purged with N<sub>2</sub> for half an hour until a clear homogeneous mixture was observed. The solution was heated to 50°C and then

the initiator K<sub>2</sub>S<sub>2</sub>O<sub>8</sub> was added with the concentration 0.1 wt % relative to the total monomer feed. The polymerization proceeded for 12 h, after which the reaction mixture was diluted with 10 volumes of distilled water, followed by precipitation into two volumes of reagent-grade acetone while stirring. The polymers were washed with acetone twice and extracted with ethanol for two days to remove all traces of water, surfactant, residual monomers, and initiator. Finally, the polymers recovered by filtration were dried under reduced pressure at 50°C for three days.

Under the same experimental conditions, as mentioned earlier, the copolymer of NaAMPS with AM was synthesized in the absence of BST and then was purified.

### Elemental analysis

The elemental analysis of the polymers was conducted by CARLO ESRA-1106 elemental analyzer (Italy) to determine carbon, nitrogen, and sulfur content. The molar compositions of P(AM-NaAMPS) and PASA used in this study were obtained by the elemental analysis of the carbon, nitrogen, and sulfur content, which are AM : NaAMPS = 84.27 : 15.73 and AM : NaAMPS : BST = 82.62 : 14.58 : 2.8, respectively.

### UV spectral analysis

The UV spectrum was obtained with a UV-240 spectrophotometer (Shimadzu, Japan). The purified PASA polymer was dissolved in pure water and the polymer concentration was 0.1 g dL<sup>-1</sup>.

### FTIR

The FTIR spectrum was conducted with a NICOLET-560 FTIR spectrophotometer (USA), which resolution capacity was 1 cm<sup>-1</sup> and scanning number was 32. The KBr pellets were prepared with the purified polymer sample.

### <sup>1</sup>H NMR

The purified PASA copolymer solution in D<sub>2</sub>O was studied at room temperature by a 400 MHz INOVA-400 instrument (America Varian Company, USA) to determine if BST hydrophobic units are incorporated into the polymer molecules.

### Fluorescence spectroscopy

Fluorescence spectra were recorded on a Hitachi-850 spectrofluorometer (Japan) at 25°C. Pyrene was employed as a micropolarity-sensitive probe, whose concentration in the polymer solutions was  $3 \times 10^{-5}$  mol L<sup>-1</sup>. The excitation wavelength was 333 nm, and the emis-

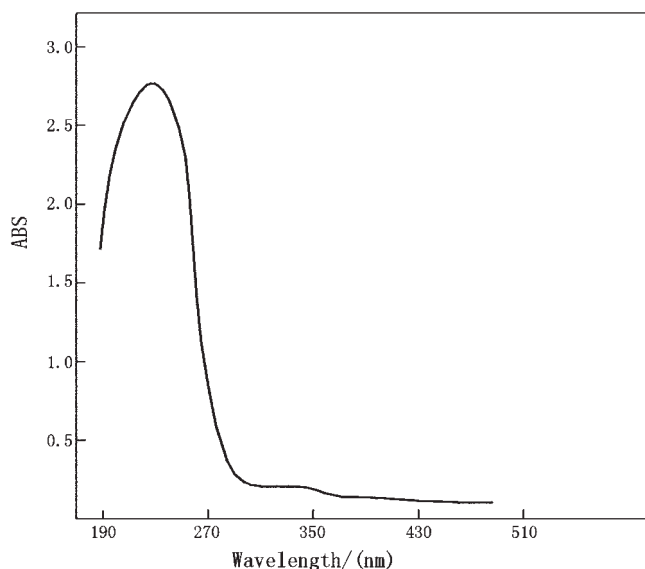


Figure 1 UV spectrum of PASA copolymer.

sion spectra were recorded between 350 and 500 nm with slit widths of 2 nm (excitation) and 3.0 nm (emission) at the scanning speed of 60 nm/min. The polymer aqueous solutions of 0.005–0.3 g dL<sup>-1</sup> were prepared by allowing the polymer to dissolve in the distilled water.

#### Atomic force microscope measurement

The atomic force micrographs were made by SPA400 AFM (Seiko, Japan), and all measurements were performed in tapping mode. All samples were covered on the mica flakes and dried naturally.

#### Environmental scanning electron microscope

The natural aggregating morphology of the hydrophobically associating polymer molecules in aqueous and brine solutions were observed by ESEM XL30 (PHILIPS, Holland). The polymer solution samples were put directly into the sample room where the temperature was maintained at -3.5°C and the pressure was controlled below 5 Torr to keep samples under solution state during the whole observation.

#### Solution viscosity measurement

Polymer solutions were prepared by dissolving the purified polymer in the distilled water or NaCl aqueous solution. The apparent viscosities of the polymer solutions were measured with a Brookfield DVIII R27112E viscometer at the shear rate of 6 s<sup>-1</sup> at 25°C.

## RESULTS AND DISCUSSION

#### Characterization of PASA

Figure 1 displays the UV spectrum of PASA. The characteristic absorption peak at 230 nm attributed to the phenyl group proves that BST hydrophobic units are incorporated into the polymer molecules.

The typical FTIR spectrum of the PASA copolymer is shown in Figure 2. The characteristic FTIR absorption peaks of PASA are as follows: -NH stretch, 3433 cm<sup>-1</sup>; C=O stretch, 1647 cm<sup>-1</sup>; -CH<sub>3</sub>, -CH<sub>2</sub>, -CH stretch, 2928, 2863, and 2787 cm<sup>-1</sup>; -CH<sub>3</sub>, -CH<sub>2</sub>, -CH bending, 1455, 1354, and 1325 cm<sup>-1</sup>; =C-H in phenyl stretch, 3090.39 cm<sup>-1</sup>; =C=C- in phenyl stretch, 1647 cm<sup>-1</sup> (overlap with C=O), 1455 cm<sup>-1</sup> (overlap

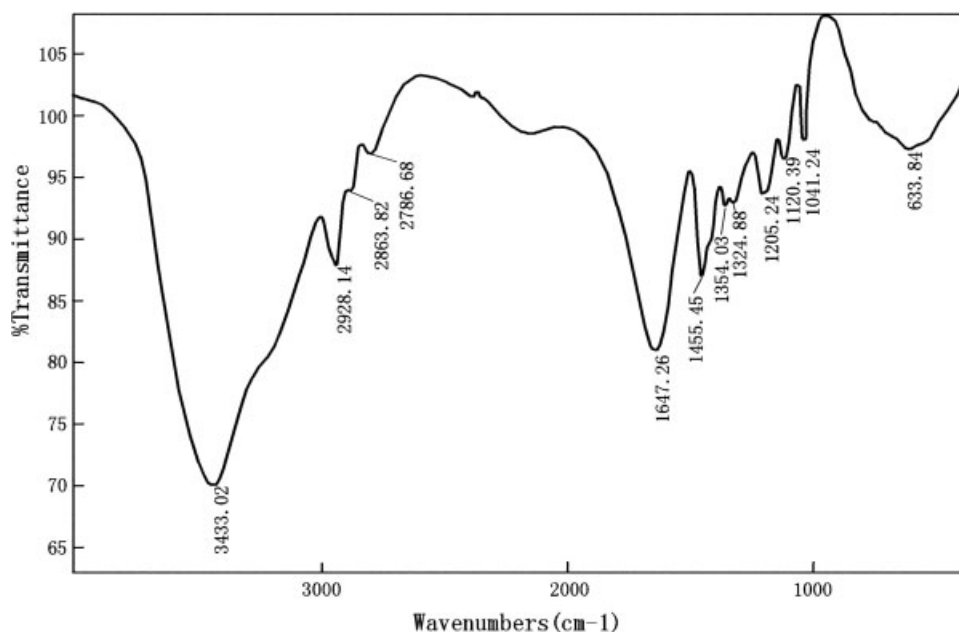


Figure 2 IR spectrum of PASA copolymer.

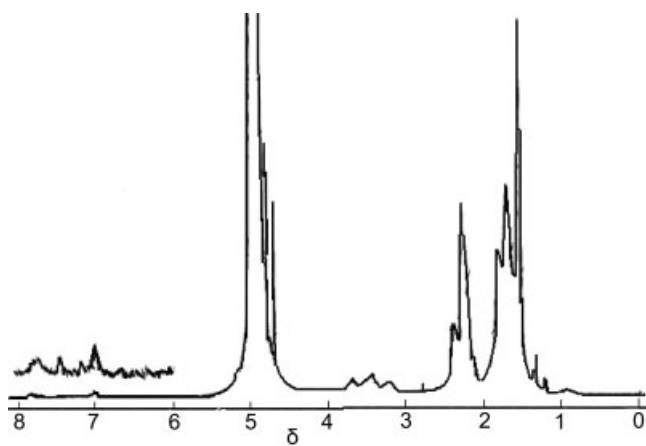


Figure 3  $^1\text{H}$  NMR spectrum of PASA copolymer.

with  $-\text{CH}_3$ ,  $-\text{CH}_2-$  bending);  $-\text{SO}_3^-$ : 1205, 1120, 1041, and  $634\text{ cm}^{-1}$ .

Figure 3 presents the  $^1\text{H}$  NMR spectrum of PASA in  $\text{D}_2\text{O}$ . All the resonances of protons are as follows: 4H ( $-\text{CH}$  of phenyl),  $\delta$  7.028–7.787 ppm; 2H ( $-\text{CH}_2$  of BST main-chain),  $\delta$  2.105 ppm; 1H ( $-\text{CH}$  of BST main-chain),  $\delta$  2.772 ppm; 6H ( $-\text{CH}_3$  of NaAMPS side chain),  $\delta$  1.674 ppm; 2H ( $-\text{CH}_2$  of AMPS side chain),  $\delta$  3.439 ppm; 2H ( $-\text{CH}_2$  of NaAMPS main chain),  $\delta$  1.781 ppm; 1H ( $-\text{CH}$  of AMPS main chain),  $\delta$  2.355 ppm; 2H ( $-\text{CH}_2$  of AM main chain),  $\delta$  1.500 ppm; 1H ( $-\text{CH}$  of AM main chain),  $\delta$  2.246 ppm; H ( $-\text{NH}_2$  of AM side chain and  $-\text{NH}$  of AMPS side chain),  $\delta$  4.716–4.967 ppm. The results show that the synthesized product is the terpolymer of AM, BST, and NaAMPS.

### Hydrophobic association probed by pyrene

Pyrene is widely used as a fluorescent probe as its solubility in water is very poor (about  $1.0 \times 10^{-7}$  mol

$\text{L}^{-1}$ ), preferably solubilized into hydrophobic microdomains and among the various fluorescent probes, pyrene is most sensitive to the change in the vibrational fine structure of its emission spectrum.<sup>17,18</sup> The  $I_1/I_3$  intensity ratio of the first (375 nm) to the third (384 nm) vibronic peaks in the fluorescence emission spectrum of pyrene is sensitive to the polarity of the local microenvironment of the pyrene probe. Thus, the formation of hydrophobic microdomains in aqueous solution can be evidenced by a decrease in the  $I_1/I_3$  ratio. Figure 4 shows the pyrene emission spectra in water and  $0.05\text{ mol L}^{-1}$  SDS aqueous solution. The  $I_1/I_3$  value decreases from about 1.76 in water to about 1.05 in  $0.05\text{ mol L}^{-1}$  SDS solution, where the pyrene probe is located in the micellar aggregates.

### P(AM-NaAMPS)

Figure 5 displays the pyrene emission spectra in P(AM-NaAMPS) aqueous solution of various polymer concentration. The  $I_1/I_3$  value is 1.75 at  $0.1\text{ g dL}^{-1}$  and almost equivalent to that measured in pure water (1.76), indicating that in such polymer solution, pyrene locates in the microenvironment similar to that in water. However,  $I_1/I_3$  decreases slightly to 1.72 at the higher concentration of  $0.2\text{ g dL}^{-1}$ , which reflects a slight hydrophobicity of the polymer backbones, leading to the increase in local concentration of pyrene in domains formed by the aggregation of molecular chains via the interaction of hydrogen bonding. The result shows that almost no hydrophobic microdomains are formed in P(AM-NaAMPS) aqueous solution.

### PASA copolymer

The pyrene emission spectra for the PASA polymer in aqueous solution and  $0.256\text{ mol L}^{-1}$  NaCl solution are

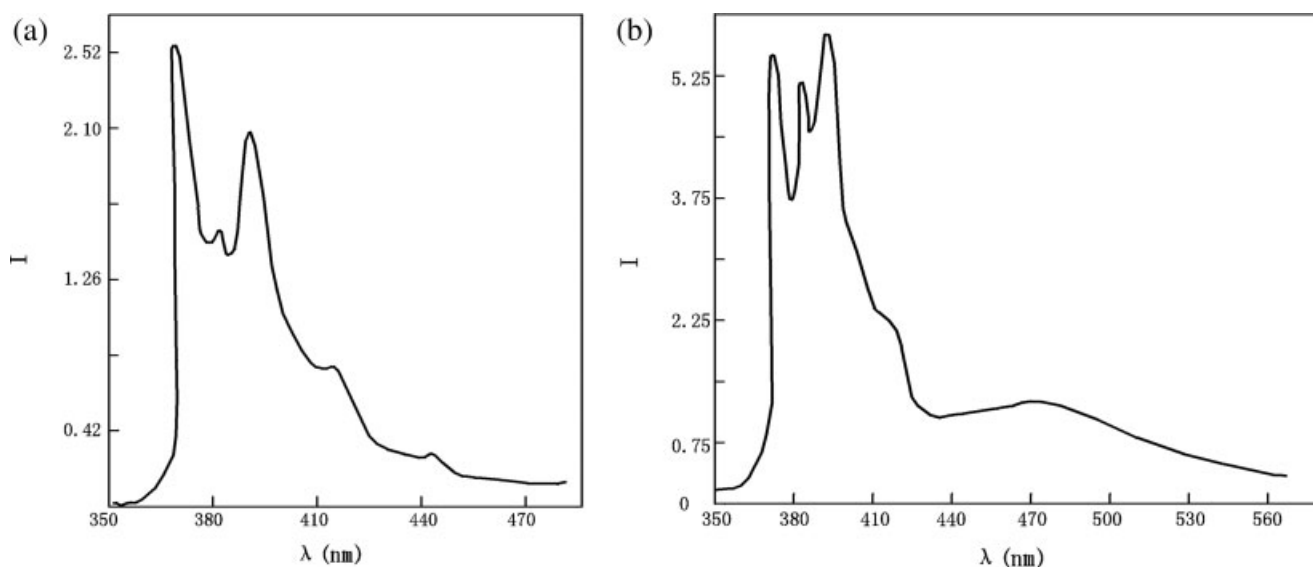
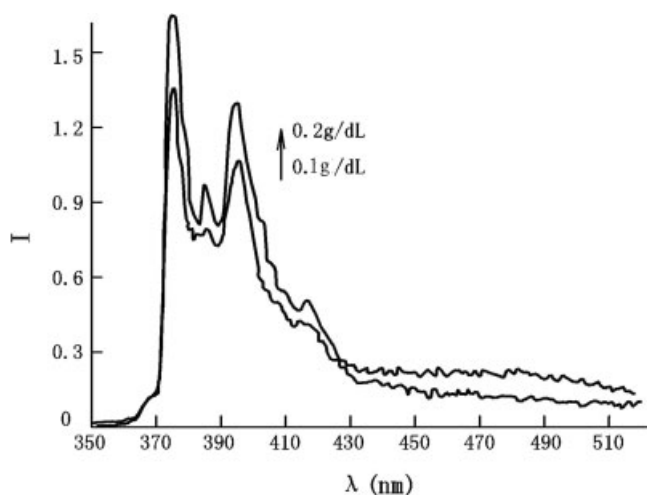


Figure 4 The pyrene emission spectra in various solution. (a)  $\text{H}_2\text{O}$  and (b)  $0.05\text{ mol L}^{-1}$  SDS.





**Figure 5** The fluorescence spectra of pyrene in the aqueous solution of P(AM-NaAMPS) at various concentration.

shown in Figures 6 and 7, respectively. Figure 8 displays the variation of  $I_1/I_3$  of pyrene as a function of polymer concentration for PASA in aqueous solution. The  $I_1/I_3$  value at the polymer concentration ( $C_p$ ) of  $0.005 \text{ g dL}^{-1}$  is 1.76, indicating that no hydrophobic microdomains exist in the polymer solution, where there are only monomolecules. The  $I_1/I_3$  value decreases with the increase in polymer concentration, and above  $0.05 \text{ g dL}^{-1}$  polymer concentration, which can be determined as the critical transition point consistent with the viscosity result, the  $I_1/I_3$  value decreases slightly. The result reveals that with the increase in polymer concentration, association hydrophobic domains increase and become more compact, leading to the increase in nonpolarity of the pyrene microenvironments, and at  $C_p = 0.3 \text{ g dL}^{-1}$ , the degree of intermolecular association reaches the plateau. Figure 9 shows the effect of polymer concentration on apparent viscosity for PASA aqueous solu-

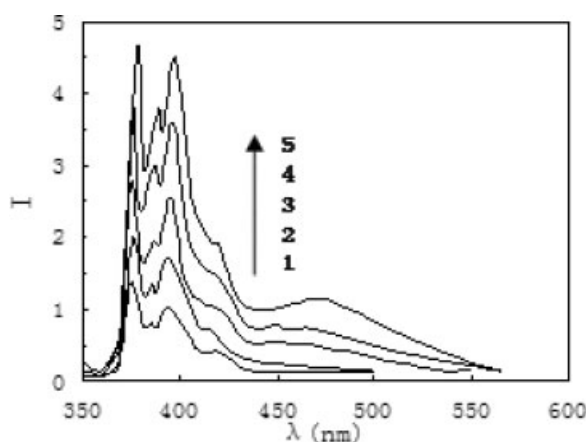


**Figure 6** The fluorescence spectra of pyrene in PASA aqueous solution at various polymer concentration. 1 : 0.005, 2 : 0.05, 3 : 0.1, 4 : 0.2, and 5 :  $0.3 \text{ g dL}^{-1}$ .

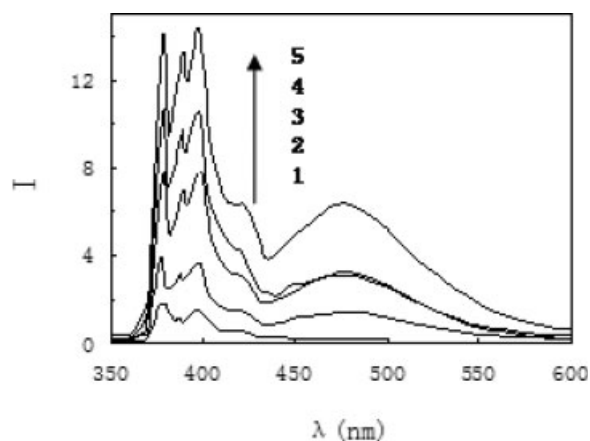


**Figure 7** The fluorescence spectra of pyrene in the  $0.256 \text{ mol L}^{-1}$  NaCl solution of PASA at various polymer concentration. 1 : 0.005, 2 : 0.05, 3 : 0.1, 4 : 0.2, and 5 :  $0.3 \text{ g dL}^{-1}$ .

tion. As exhibited in Figure 9, the critical association concentration is  $0.05 \text{ g dL}^{-1}$  as with increasing polymer concentration, the apparent viscosity increases slowly below  $0.05 \text{ g dL}^{-1}$ , and then increases dramatically. The fluorescent probe and viscosity measurements show that with increasing polymer concentration, above  $0.05 \text{ g dL}^{-1}$  PASA, although the nonpolarity of the hydrophobic microdomains tend gradually to be constant, the microdomains and viscosity increase abruptly because of the remarkable increase of aggregates.

In  $0.256 \text{ mol L}^{-1}$  NaCl solution, the change of  $I_1/I_3$  with the polymer concentration is almost the same as that in the aqueous solution. But, at the same polymer concentration, the  $I_1/I_3$  value in brine solution is apparently lower than that in the aqueous solution, which indicates that the hydrophobic domains become more compact, leading to the increase in nonpolarity of pyrene environments. At  $C_p = 0.005 \text{ g dL}^{-1}$ , the  $I_1/I_3$  value is about 1.64 and lower than that in

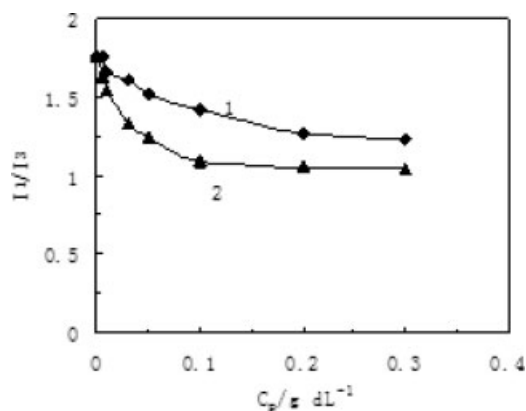


**Figure 8** The  $I_1/I_3$  values of pyrene as a function of PASA concentration. (1) Pure water; (2)  $0.256 \text{ mol L}^{-1}$  NaCl solution.

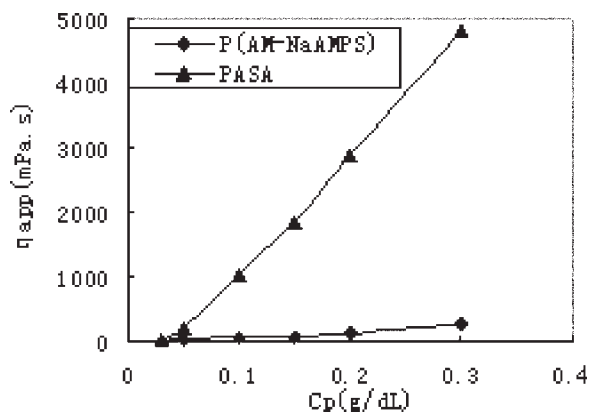


**Figure 9** Effect of polymer concentration on the apparent viscosity of copolymer aqueous solution.

pure water and the polymer aqueous solution, which shows that in the very dilute solution, the intramolecular associations are reinforced because of the electrostatic shielding of  $\text{Na}^+$  on  $-\text{SO}_3^-$  groups in the polymer chains, resulting in the formation of a small amount of condensed hydrophobic domains. The  $I_1/I_3$  value dramatically decreases below  $0.05 \text{ g/dL}$  concentration, and gradually drops to 1.08 at the higher concentration of  $0.1 \text{ g/dL}$ . Finally, the  $I_1/I_3$  value reaches 1.05 at  $C_p = 0.3 \text{ g/dL}$ , indicating that the polarity of pyrene microenvironment for this case equals that in  $0.05 \text{ mol L}^{-1}$  SDS aqueous solution.

The fluorescence emission spectrum of the excited pyrene in the absence of pyrene–pyrene interactions (monomer emission having intensity  $I_m$ ) consist of major peaks at 375, 384, and 399 nm. Excimer formation occurs when the concentration of pyrene in the hydrophobic microenvironment is high enough for an excited pyrene ( $\text{Py}^*$ ) and a pyrene in its ground state to come into close proximity during the  $\text{Py}^*$  lifetime. Pyrene excimer emission (intensity  $I_e$ ) is characterized

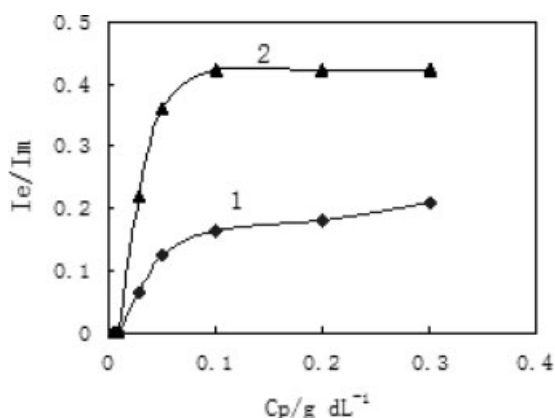


**Figure 10** The  $I_e/I_m$  values of pyrene as a function of PASA concentration. (1) Pure water; (2)  $0.256 \text{ mol L}^{-1}$  NaCl solution.

by a broad featureless spectral emission peak centered at 475 nm. Hence, the  $I_e/I_m$  ratio has often been used as an indicator of the degree of interaction between fluorophores.<sup>19</sup> For hydrophobically associating polymer, the  $I_e/I_m$  ratio provides a measure to characterize the association degree of hydrophobic segments on the polymer chains. Figure 10 shows a plot of  $I_e/I_m$  versus polymer concentration in the aqueous and  $0.256 \text{ mol L}^{-1}$  NaCl solution, respectively. Above  $0.01 \text{ g dL}^{-1}$  polymer concentration, the excimers start to form for PASA in the aqueous and brine solution. In the aqueous solution, the  $I_e/I_m$  ratio increases with the increase in polymer concentration and reaches 0.21 at  $C_p = 0.3 \text{ g dL}^{-1}$ . However, in  $0.256 \text{ mol L}^{-1}$  NaCl solution, the  $I_e/I_m$  value abruptly increases to 0.42 with the increase in concentration to  $0.1 \text{ g dL}^{-1}$ , and then it tends to be constant. At any polymer concentration higher than  $0.01 \text{ g dL}^{-1}$ , intra- or intermolecular association of hydrophobic groups in the brine solution is much stronger than that in the aqueous solution. The above-mentioned results reveal that by the addition of NaCl, hydrophobic aggregates become more compact because of the electrostatic shielding effect of intermolecular repulsion, leading to the great increase in the solubility of pyrene in hydrophobic domains.

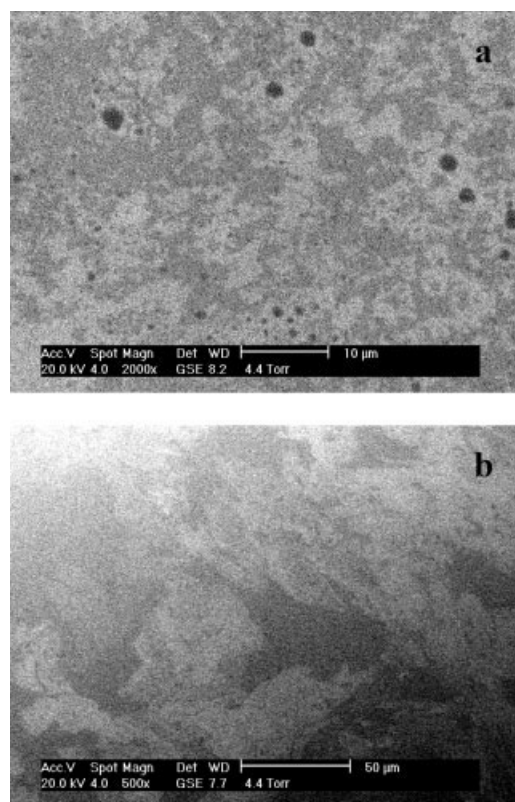


**Figure 11** The ESEM images of PASA in aqueous solution at various polymer concentration. (a)  $0.03 \text{ g dL}^{-1}$ ; (b)  $0.05 \text{ g dL}^{-1}$ .

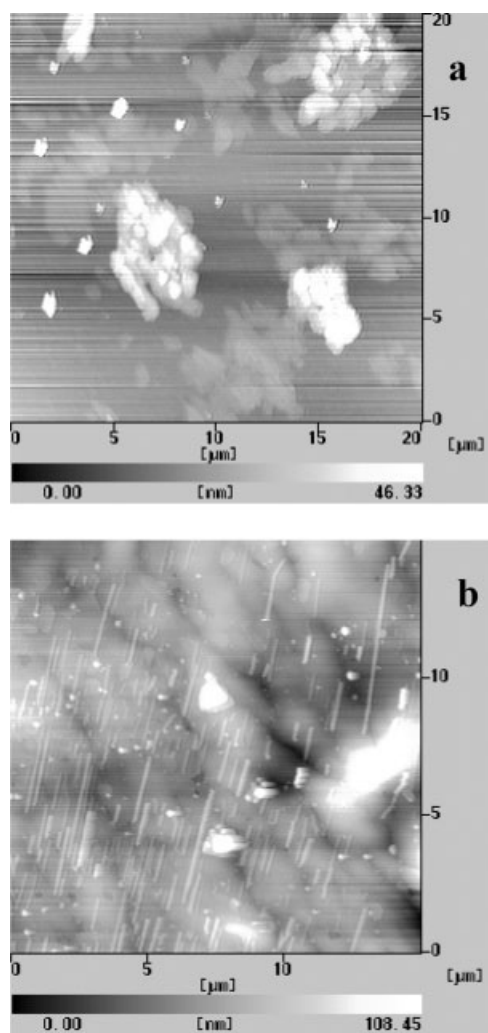


**Figure 12** The AFM images of  $0.03 \text{ g dL}^{-1}$  and  $0.05 \text{ g dL}^{-1}$  PASA aqueous solution. (a)  $0.03 \text{ g dL}^{-1}$  and (b)  $0.05 \text{ g dL}^{-1}$ .

### The associating morphologies of the copolymer in aqueous solutions

#### $0.03 \text{ g dL}^{-1}$ and $0.05 \text{ g dL}^{-1}$ PASA

Figure 11(a) shows aggregation morphology of  $0.03 \text{ g dL}^{-1}$  PASA aqueous solution. Although the images are not very clear due to the low concentration, numerous hydrophobic aggregates with different sizes are observed in the images (undersurface aggregates are displayed as black blocks in ESEM images), resulting in the viscosity of  $42 \text{ mPa s}$  for  $0.03 \text{ g dL}^{-1}$  PASA solution. With the increase in polymer concentration to  $0.05 \text{ g dL}^{-1}$ , the aggregate morphologies become more huge [Fig. 11(b)], leading to the remarkable increase in viscosity from  $42$  to  $203 \text{ mPa s}$ , indicative of intermolecular hydrophobic association. The results are consistent with those of fluorescent probe and AFM, and reflect that the critical associating concentration of such polymer in aqueous solution is about  $0.05 \text{ g dL}^{-1}$ . As shown in Figure 12(a,b), with increasing polymer concentration from  $0.03$  to  $0.05 \text{ g dL}^{-1}$

$\text{dL}^{-1}$ , the aggregate morphologies change from separated aggregates to continuous network distributed in the aqueous solution.

#### $0.1 \text{ g dL}^{-1}$ PASA

Figure 13 shows associative morphologies of  $0.1 \text{ g dL}^{-1}$  PASA in aqueous solution. The integrated three-dimensional networks are formed due to the intermolecular hydrophobic association [Fig. 13(a)]. The result is consistent with the AFM measurement (Fig. 14). However, the network bones are very thin. On the other hand, there are flower-like associating blocks on knots of network [Fig. 13(b)].

#### $0.2 \text{ g dL}^{-1}$ PASA

When the sample at the room temperature was directly put in the sample room at  $-3.5^\circ\text{C}$ , water on the sample surface volatilized rapidly, and the morphology of the polymer was shown in Figure 15(a). Also, the network bones of the polymer became apparently bigger (diameter:  $2\text{--}4 \mu\text{m}$ ) and more compact for  $0.2 \text{ g dL}^{-1}$  PASA. The pressure in the sample room increased highly in contrast to the saturated vapor pressure of the measuring temperature, and the surface of the sample was covered by water, and then the measured pressure decreased gradually until

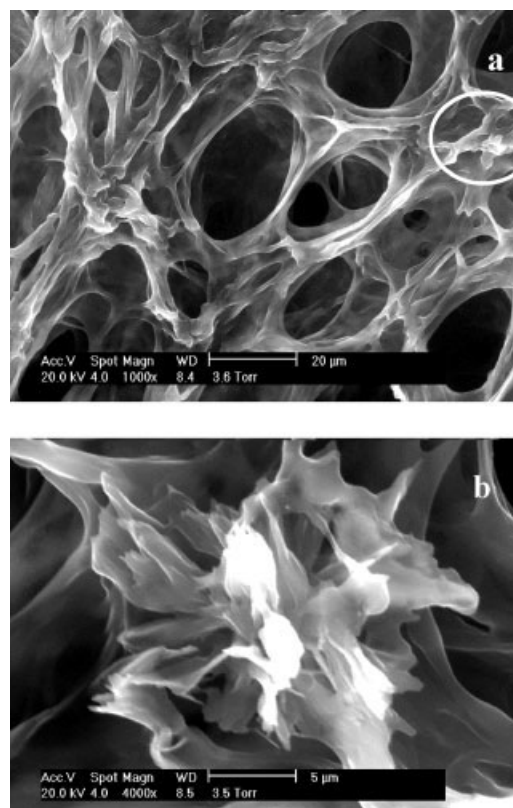


**Figure 13** The ESEM images of PASA in aqueous solution at the concentration of  $0.1 \text{ g dL}^{-1}$ .



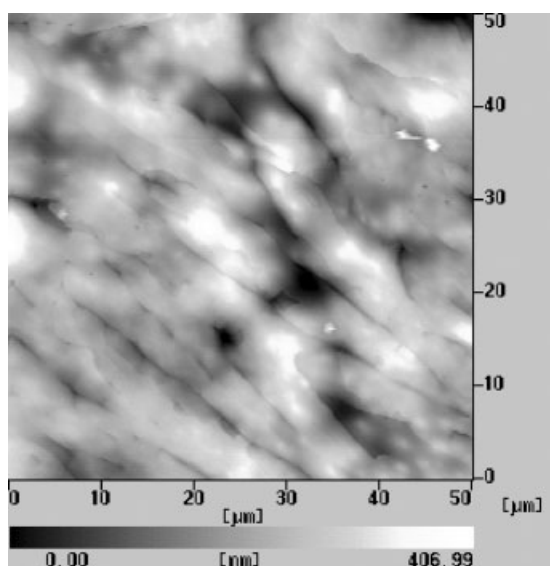


**Figure 14** The AFM images of  $0.1 \text{ g dL}^{-1}$  PASA aqueous solution.

4.9 Torr, the network structures were still in water [Fig. 15(b)]. With the increase in the polymer concentration from  $0.1$  to  $0.2 \text{ g dL}^{-1}$ , the intermolecular associations are reinforced; charge–charge repulsions act to expand the polymer molecules and are not suffi-

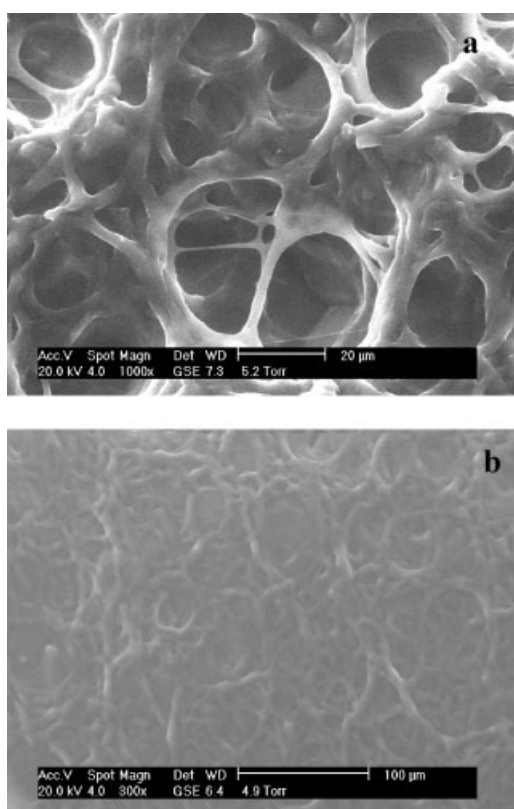


**Figure 15** The ESEM images of PASA in aqueous solution at the concentration of  $0.2 \text{ g dL}^{-1}$ .

cient to disrupt hydrophobic interactions, resulting in the abrupt increase in viscosity from  $1020$  to  $2900 \text{ mPa s}$ .

#### $0.3 \text{ g dL}^{-1}$ and $0.5 \text{ g dL}^{-1}$ PASA

Figure 16 shows the ESEM images of  $0.3$  and  $0.5 \text{ g dL}^{-1}$  PASA aqueous solution. The diameters of the networks bones are  $2.5\text{--}5$  and  $5\text{--}15 \mu\text{m}$ , respectively. The results of ESEM measurements suggest that with the increase in the polymer concentration in the range of  $0.1\text{--}0.5 \text{ g dL}^{-1}$ , the network structures of the polymer become much more huge and condensed, which leads to the improvement of the apparent viscosity from  $1020 \text{ mPa s}$  at  $C_p = 0.1 \text{ g dL}^{-1}$  to  $11,832 \text{ mPa s}$  at  $C_p = 0.5 \text{ g dL}^{-1}$ , and excellent thickening property of PASA in aqueous solution is due to integrated network structures.

The measurement conditions of ESEM are different from those of solution viscosity, but with the increase in the polymer concentration, the change of associating morphologies accords with that of solution viscosity, which is clarified by the above-mentioned results, and shows that the viscosification properties of hydrophobically associating polymers are depended on the associative structures. The fluorescent probe results and the ESEM images show that, for PASA aqueous

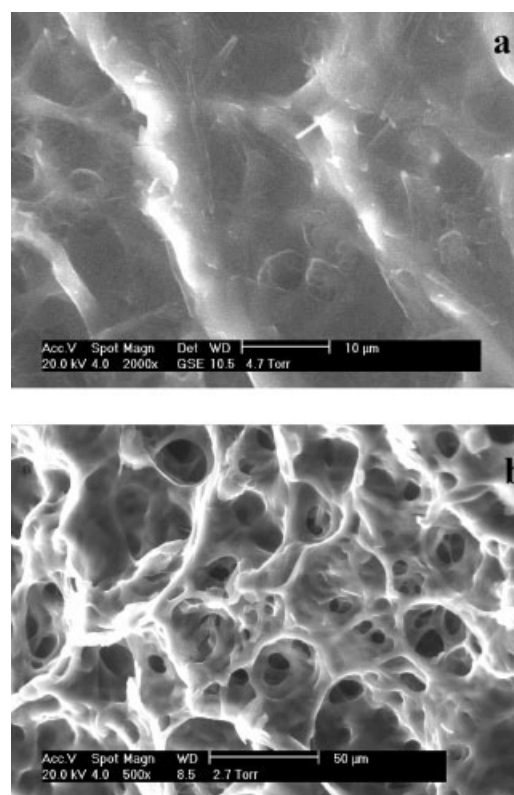


**Figure 16** The ESEM images of PASA in aqueous solution at various polymer concentration. (a)  $0.3 \text{ g dL}^{-1}$  and (b)  $0.5 \text{ g dL}^{-1}$ .



solution, with increasing polymer concentration from 0.1 to 0.5 g dL<sup>-1</sup>, the associating network structures become bigger and compact because of more hydrophobic groups participating in intermolecular association, leading to the remarkable increase in solution viscosity and the increase in the local concentration of pyrene in associating microdomains resulting in the increase of  $I_e/I_m$  from 0.164 to 0.210, but nonpolarity of hydrophobic domains change slightly as the hydrophobic interactions between chains may be almost attain balance with the intermolecular electrostatic repulsions between  $-\text{SO}_3^-$  groups.

### The associating morphologies of the copolymer in brine solution

#### Different NaCl concentration

As shown in Figure 17(a,b), for 0.2 g dL<sup>-1</sup> PASA in 0.085 mol L<sup>-1</sup> NaCl aqueous solution, the overlapped continuous networks spanned in aqueous solution are collapsed by the addition of a small amount of salt. Lots of condensed aggregates with different sizes and shapes are formed, resulting in the decrease in solution viscosity. However, with the increase in NaCl concentration from 0.085 to 0.256 mol L<sup>-1</sup>, the number and the size of aggregates increase obviously [Fig. 18(a,b)], and the apparent viscosity increase

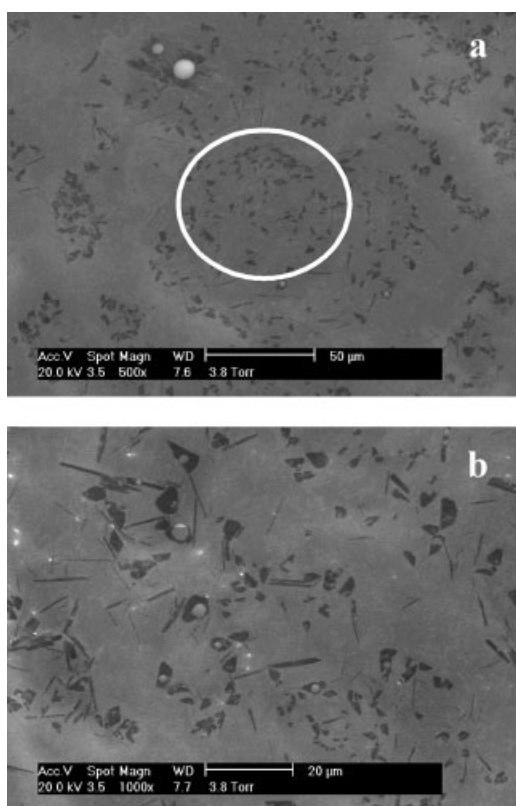


**Figure 17** The ESEM images of PASA in 0.085 mol L<sup>-1</sup> NaCl aqueous solution. Polymer concentration: 0.2 g dL<sup>-1</sup>.

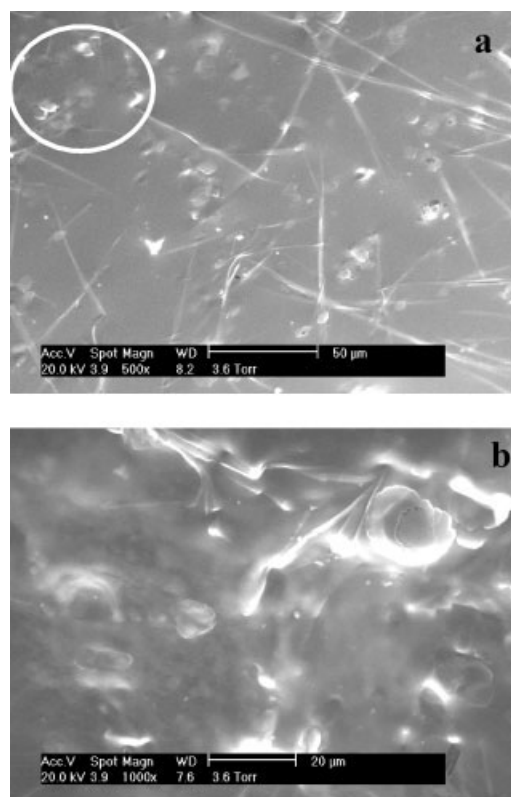


**Figure 18** The ESEM images of PASA in 0.256 mol/L NaCl aqueous solution. Polymer concentration: 0.2 g dL<sup>-1</sup>.

from 72 to 108 mPa s, indicating that intermolecular associations of hydrophobic groups are strengthened.

#### Different polymer concentration

Figure 19 shows the morphologies of the polymer for 0.5 g dL<sup>-1</sup> PASA in 0.256 mol L<sup>-1</sup> NaCl solution, in which (a) and (b) are the morphologies of different positions of the sample and (c) is the amplified images for (b). By comparison with Figure 18, with the increase in polymer concentration in the brine solution, the number and sizes of aggregates increase obviously, resulting in the increase in apparent viscosity from 108 to 7092 mPa s, which is the same as the case in the pure water. Nevertheless, continuous associative network structures are still not observed in the brine solution with so high polymer concentration.

The ESEM images and fluorescent probe results when compared with PASA aqueous solution show that aggregates in brine solution become more compact by the addition of NaCl, leading to more pyrene excimers caused by the increase in concentration of pyrene in hydrophobic domains. The results also suggest that the suitable association degree of hydrophobic groups can result in high solution viscosity and, on the contrary, too strong hydrophobic interaction of chains is not favorable to the viscosification of hydrophobically associating water-soluble polymers. In ad-

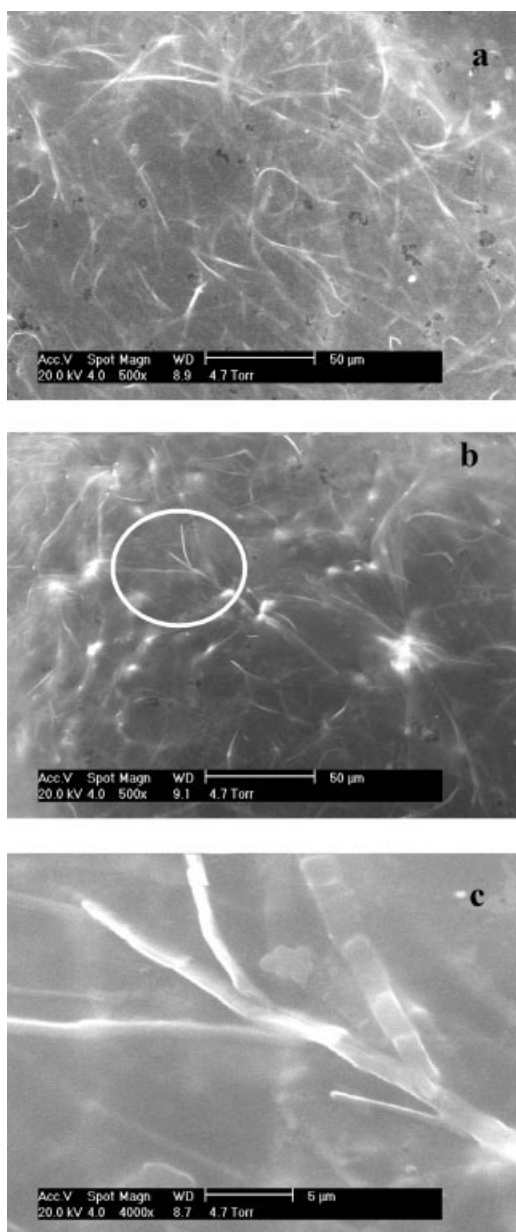


**Figure 19** The ESEM images of PASA in 0.256 mol/L NaCl aqueous solution. Polymer concentration:  $0.5 \text{ g dL}^{-1}$ .

dition, although the number and sizes of aggregates increase with the increase in the polymer concentration above  $0.1 \text{ g dL}^{-1}$ , the association degree and nonpolarity of aggregates tend to be constant.

### CONCLUSIONS

The terpolymer (PASA) with AM, BST, and NaAMPS was synthesized by micellar free radical copolymerization in distilled water using SDS as the surfactant and potassium persulphate as the free radical initiator. The synthesized product was characterized by elemental analysis, UV, FTIR, and  $^1\text{H}$ NMR. The flour-

escent probe analysis indicates that the PASA molecules have strong hydrophobically associating effects in pure water and NaCl solution, the hydrophobic microstructures turn more compact by the addition of NaCl, and with the increase in PASA concentration at low concentrations, the nonpolarity of hydrophobic microdomains increase in the aqueous and brine solution and tends to be constant above  $0.2 \text{ g dL}^{-1}$  PASA. The clear ESEM images of integrated network-structures of hydrophobically associating water-soluble copolymer in aqueous solution were obtained. ESEM measurements show that gigantic aggregates have been formed in the aqueous solution of  $0.05 \text{ g dL}^{-1}$  PASA, indicating that the critical association concentration of the polymer is about  $0.05 \text{ g dL}^{-1}$ , and with the increase in PASA concentration, the network structures become much more huge and condensed. The network-structures of PASA are disrupted by the addition of salt, and condensed spherical, column-like clusters are formed, leading to the decrease in apparent viscosity of PASA solution. However, with the increase in NaCl concentration or PASA concentration, the number and size of aggregates increase apparently because of reinforced intermolecular hydrophobic association, resulting in the remarkable increase in apparent viscosity of PASA solution. These results reveal the viscosifying mechanisms of the polymer in the aqueous solution and salt solution, which are consistent with the AFM and viscosity study results.

### References

- Hutchinson, B. H.; McCormick, C. L. *Polymer* 1986, 27, 623.
- McCormick, C. L.; Kramer, M. C.; Chang, Y.; Branham, K. D.; Kathmann, E. L. *Polym Prepr* 1993, 34, 1005.
- Dragan, S.; Ghimici, L. *Polymer* 2001, 42, 2886.
- McCormick, C. L.; Nonaka, T.; Johnson, C. B. *Polymer* 1988, 29, 731.
- Ye, L.; Luo, K.; Huang, R. *Eur Polym J* 2000, 36, 1711.
- Ye, L.; Mao, L.; Huang, R. *J Appl Polym Sci* 2001, 82, 3552.
- Mondet, J.; Lion, B. *Eur. Pat. Appl.* 494,022 (1992).
- McCormick, C. L.; Middleton, J. C.; Cummins, D. F. *Macromolecules* 1992, 25, 1201.
- Busse, K.; Kressler, J. *Macromolecules* 2002, 35, 178.
- Stahl, G. A.; Schulz, D. N. *Water-Soluble Polymers for Petroleum Recovery*; Plenum: New York, 1988.
- Waterson, A. C.; Haralaba Kopopulos, A. A. *Polym Prepr* 1992, 33, 278.
- Zhong, C.; Huang, R.; Ye, L.; Dai, H. *J Appl Polym Sci* 2006, 101, 3996.
- Huang, R.; Zhong, C. *China Pat.* 154,2031 (2004).
- Littke, A. F.; Schwarz, L. F.; Gregory, C. *J Am Chem Soc* 2002, 124, 6343.
- Hill, A.; Candau, F.; Selb, J. *Macromolecules* 1993, 26, 4521.
- Ma, J.; Cui, P.; Zhao, L.; Huang, R. *Eur Polym J* 2002, 38, 1627.
- Wilhelm, M.; Zhao, C. L.; Wang, Y. *Macromolecules* 1991, 24, 1033.
- Chen, J.; Jiang, M.; Zhang Y.; Zhou, H. *Macromolecules* 1999, 32, 4816.
- Winnik, F. M. *Chem Rev* 1993, 93, 587.